730 Journal of Electrical Engineering & Technology Vol. 7, No. 5, pp. 730~735, 2012
http://dx.doi.org/10.5370/JEET.2012.7.5.730

Back EMF Design of an AFPM Motor using PCB Winding by Quasi 3D Space Harmonic Analysis Method

Dae-Kyu Jang*, Jung-Hwan Chang† and Gun-Hee Jang**

Abstract – This paper presents a method to design the waveform of a back electromotive force (back EMF) of an axial flux permanent magnet (AFPM) motor using printed circuit board (PCB) windings. When the magnetization distribution of permanent magnet (PM) is given, the magnetic field in the air gap region is calculated by the quasi three dimensional (3D) space harmonic analysis (SHA) method. Once the flux density distribution in the winding region is determined, the required shape of the back EMF can be obtained by adjusting the winding distribution. This can be done by modifying the distance between patterns of PCB to control the harmonics in the winding distribution. The proposed method is verified by finite element analysis (FEA) results and it shows the usefulness of the method in eliminating a specific harmonic component in the back EMF waveform of a motor.

Keywords: Axial flux, Back electromotive force, PCB winding, Space harmonic analysis

1. Introduction

In the design of permanent magnet (PM) motor, the shape and amplitude of a back electromotive force (back EMF) are important factors influencing motor performances [1, 2]. Particularly, the unwanted harmonic components included in the back EMF generate torque ripples and losses in the motor [3]. In conventional axial flux permanent magnet (AFPM) motors, the waveform of the back EMF is mainly determined by two factors, the flux density distribution by PM in the air gap region and tooth shape of stator for confining the field to the core. However, in the slotless type motor, there are no means for guiding the magnetic flux to the winding region and it is also not possible to design the shape of the back EMF by changing the tooth shape for a given PM flux.

This paper presents a method to design the shape of the back EMF waveform of an AFPM motor using printed circuit board (PCB) windings. Fig. 1 shows the procedure of the proposed method using the quasi three dimensional space harmonic analysis (3D SHA) method, which is one of analytical techniques to predict the magnetic field distribution in the motor [4]. When the magnetization distribution of PM is given, the magnetic field in the air gap region is calculated by 3D SHA method. This method is derived by combining the two dimensional space harmonic analysis (2D SHA) method and a correction function for magnetic flux in radial position by considering the reduction of magnetic field near the inner and outer radius of AFPM [5, 6]. Once the flux density distribution in the winding region is calculated, the required shape of the back EMF can be obtained by adjusting the winding distribution. It can be done by modifying the distance between patterns of the PCB to control the harmonics in the winding region. The proposed method is verified by finite element analysis (FEA) results and it shows the usefulness of the method in eliminating specific harmonic components in the back EMF waveform of a motor.

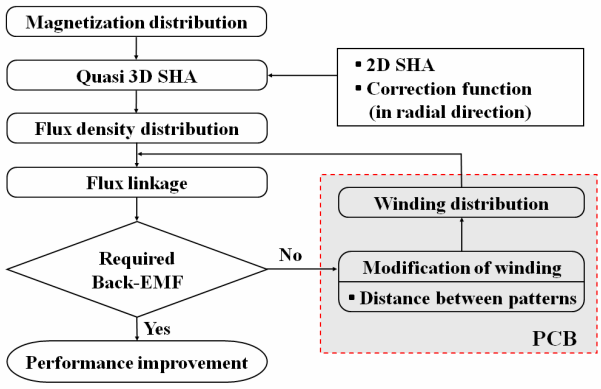

Fig. 1. Procedure to design back EMF waveform

2. Principle of the Method

2.1 2D analytical magnetic-field solution

In order to obtain magnetic field distribution produced by PM, the stator and rotor core are assumed to have infinite permeability. When a current is absent in solution region, magnetic field intensity, $\vec{H}$ can be represented using magnetic scalar potential, φ.

† Corresponding Author: Department of Electrical Engineering, Donga University, Busan, Korea. (cjhwan@dau.ac.kr)
* Department of Electrical Engineering, Donga University, Busan, Korea. (cjhwan@dau.ac.kr)
** PREM, Department of Mechanical Engineering, Hanyang University, Seoul, Korea. (ghjang@hanyang.ac.kr)
Received: January 6, 2012; Accepted: March 7, 2012

$$\vec{H} = -\vec{\nabla}\varphi \tag{1}$$

For the AFPM motor, magnetic field can be described by Laplace's equation and Poisson's equation in polar coordinates as follows.

$$\frac{1}{r^2}\frac{\partial^2\varphi_a}{\partial\theta^2} + \frac{\partial^2\varphi_a}{\partial z^2} = 0 \tag{2}$$

$$\frac{1}{r^2}\frac{\partial^2\varphi_m}{\partial\theta^2} + \frac{\partial^2\varphi_m}{\partial z^2} = \frac{\vec{\nabla}\cdot\vec{M}}{\mu_r} \tag{3}$$

where the subscripts a and m denote the air gap and PM regions respectively, r is a radius at which the magnetic field is computed, μ_r is the relative recoil permeability of the magnet, and $\vec{M}$ is magnetization distribution of PM.

Since the magnetic field distribution is an even and periodic function along circumferential direction, the solutions of Laplace's equation and Poisson's equation in the air gap and PM regions are as follows.

$$\varphi_a(\theta) = \sum_{n=1,3,5\cdots}^{\infty}\left(C_1 e^{\frac{nN_p}{r}z} + C_2 e^{-\frac{nN_p}{r}z}\right)\cos(nN_p\theta) \tag{5}$$

$$\varphi_m(\theta) = \sum_{n=1,3,5\cdots}^{\infty}\left(C_3 e^{\frac{nN_p}{r}z} + C_4 e^{-\frac{nN_p}{r}z} + C_5\right)\cos(nN_p\theta) \tag{6}$$

where θ is circumferential angle in mechanical measure and N_p is the number of pole pairs.

Specific solutions to the flux density in the air gap region are obtained by applying the customary boundary conditions which specify that the tangential component of field intensity and the normal component of the flux density are continuous across material boundaries.

$$B_{a\theta}(\theta) = \mu_0 H_{a\theta} = -\mu_0\frac{1}{r}\frac{\partial\varphi_a}{\partial\theta} = \sum_{n=1,3,5\cdots}^{\infty} B_{a\theta n}\sin(nN_p\theta) \tag{7}$$

$$B_{az}(\theta) = \mu_0 H_{az} = -\mu_0\frac{\partial\varphi_a}{\partial z} = \sum_{n=1,3,5\cdots}^{\infty} B_{azn}\cos(nN_p\theta) \tag{8}$$

In order to consider the finite permeability and saturation characteristic of the ferromagnetic materials, a factor, C_r is introduced. It is defined by the ratio of magnetic flux densities at the air gap region in the equivalent magnetic circuit with and without considering reluctance of the core [1]. It is a constant slightly greater than one and decreases the magnetic flux density in the winding region to compensate for assumption of infinite permeability of the core in the SHA method.

2.2 3D analytical magnetic-field solution

In the 2D SHA, the flux density is assumed to have uniform value in the radial direction. However, in reality, the flux density is rapidly decreasing near the inner and outer radius of the AFPM. This effect can be considered by fallowing correction function derived from the 3D FEA [6]. It shows the normalized axial flux density distribution according to the radial position of a motor as shown in Fig. 2.

$$G(r) = \frac{1}{\pi}\left\{\text{atan}\left(\frac{r-r_i}{a}\right) - \text{atan}\left(\frac{r-r_o}{a}\right)\right\} \tag{9}$$

$$a = \frac{\beta_1(r_o - r_i)}{\tan(\beta_2\pi/2)} \tag{10}$$

where r_i and r_o are the inner and outer radius of the AFPM motor. β_1 and β_2 are correction factors. β_1 is used to define the effective radius and β_2 is used to adjust the drop of the axial flux density near the inner and outer radius of the AFPM motor.

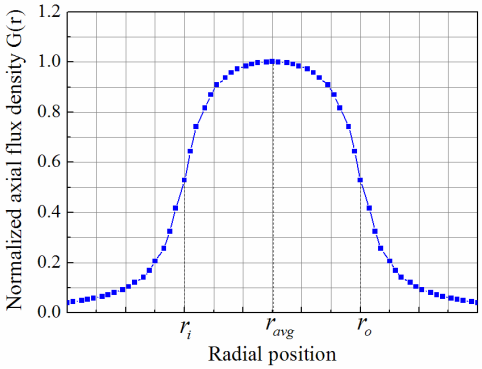

Fig. 2. Axial flux density according to radial position

2.3 Winding distribution

With the information on the flux density in the winding region, PCB patterns can be designed to have appropriate winding distribution that decreases specific harmonic components in the back EMF waveform. Unlike the conventional winding layouts such as concentric and distributed winding, the winding distribution by PCB can be adjusted by modifying the intervals of each pattern as shown in Fig. 3. Finally, the windings distribution is described by following the Fourier series.

$$N(r,\theta) = N\cdot N(r)\cdot N(\theta) \tag{11}$$

$$N(r) = \sum_{m=1,3,5\cdots}^{\infty} N_{rm}\cos(mr), N(\theta) = \sum_{k=1,3,5\cdots}^{\infty} N_{\theta k}\cos\left(\frac{kN_c}{2}\theta\right) \tag{12}$$

where N is the number of turns, N_c is the number of coils, and, $N(r)$ and $N(\theta)$ are normalized winding distribution in radial and circumferential direction, respectively. Unlike $N(r)$ having constant pattern distance, $N(\theta)$ has variable pattern distance to control the shape of the back EMF.

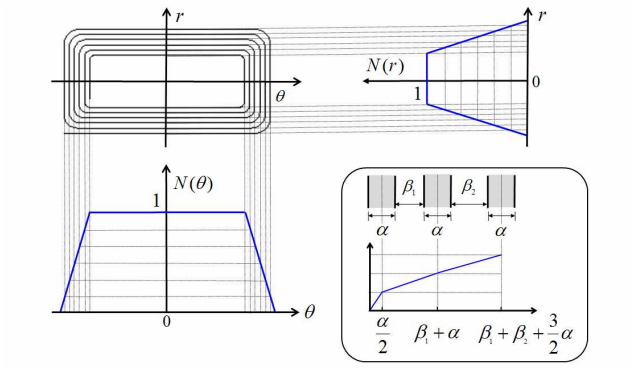

Fig. 3. Winding distribution in radial and circumferential direction

2.4 Back EMF

From the flux density and winding distribution, the flux linkage in a coil is given as

$$\lambda(\alpha) = \int_{-\frac{\theta_c}{2}}^{\frac{\theta_c}{2}} \int_{r_i}^{r_o} N(r,\theta) \cdot G(r) \cdot B_{az}(\theta+\alpha) \cdot r dr d\theta \qquad (13)$$

where θ_c and α are the angular coil pitch and the rotating angle of rotor in mechanical measure, respectively.

Substituting (8), (9) and (11) into (13), the flux linkage expression can be arranged as

$$\lambda(\alpha) = N \cdot \int_{r_i}^{r_o} N(r) \cdot G(r) \cdot r dr \cdot \int_{-\frac{\theta_c}{2}}^{\frac{\theta_c}{2}} N(\theta) \cdot B_{az}(\theta+\alpha) d\theta$$
$$= N \cdot k_r \cdot \sum_{n=1,3,5\cdots}^{\infty} \left(\sum_{k=1,3,5\cdots}^{\infty} N_{\theta k} k_{kn} \right) B_{azn} \cdot \cos\left(nN_p\alpha\right) \qquad (14)$$

where

$$k_r = \int_{r_i}^{r_o} N(r) \cdot G(r) \cdot r dr \qquad (15)$$

$$k_{kn} = \int_{-\frac{\theta_c}{2}}^{\frac{\theta_c}{2}} \cos\left(\frac{kN_c}{2}\theta\right) \cdot \cos\left(nN_p\theta\right) d\theta \qquad (16)$$

The associated back EMF is the derivative of the flux linkage as follows.

$$e(\alpha) = NN_p\omega_m k_r \sum_{n=1,3,5\cdots}^{\infty} n \cdot kw_n B_{azn} \sin\left(nN_p\alpha\right) \qquad (17)$$

where

$$kw_n = \sum_{k=1,3,5\cdots}^{\infty} N_{\theta k} k_{kn} \qquad (18)$$

In (17), it is found that the amplitude of the nth harmonic component in the back EMF is determined by coefficients, kw_n and B_{azn}, Fourier coefficient of the axial component of the magnetic flux density in the winding region. When the air gap flux density has harmonic components, it is true in general, the back EMF waveform has harmonics even though the winding distribution is assumed to have pure sine wave. Thus, each harmonic component of the back EMF can be eliminated only when the winding distributions satisfy the following condition.

$$kw_n = \sum_{k=1,3,5\cdots}^{\infty} N_{\theta k} k_{kn} = (N_{\theta 1} k_{1n} + N_{\theta 3} k_{3n} + N_{\theta 5} k_{5n} + \cdots) = 0 \qquad (19)$$

When the numbers of pole pairs and coils are determined, the k_{kn} has constant values. Therefore, the kw_n can be zero by finding the combinations of the harmonic components in the winding distribution based on (19).

2.5 Winding design method

In order to eliminate a specific harmonic in the back EMF, each harmonic of the winding distribution could be adjusted to satisfy (19). Although there are many combinations of the harmonics making kw_n to be zero, the PCB winding could not express all of them due to the spatial harmonic distortion. To find feasible solutions satisfying (19), the general winding distribution having the same interval between the patterns is a good starting point in designing PCB patterns

In this paper, two methods are presented based on the given general winding distribution. The first method considers one winding harmonic multiplied by the biggest value of k_{kn} as design variable. With this selection, we can eliminate a certain harmonic in back EMF by the smallest change in the general winding distribution.

For limited space and the number of turns, it is difficult to express high harmonics in winding distribution. The second method consider the third winding harmonic, the lowest one, as design variable. However, one more thing should be consider in this method. If the third harmonic has too high value to satisfy (19), a distortion of the winding distribution would be severe and the designed winding could not be implemented by PCB. Thus, in order to minimize the change of the third winding harmonic, the harmonic of the general winding distribution multiplied by biggest value of k_{kn} is made to zero in the second method.

3. Application of the method

The proposed method is applied to a slotless AFPM motor having specifications as shown in Table 2. With the axial magnetization by Halbach array of PM, a coil has 5 layers and each layer has 8 turns.

In order to validate the proposed method, the waveforms of the back EMF and its harmonic components are compared with FEA as well as SHA results. In the general 3D FEA,

each coil is modeled as a single tube not distinguishing conductors for convenience. However, with this method, it is not possible to analyze the effect of the winding layout having different interval between conductors on the waveform of the back EMF. In this paper, the PCB patterns are modeled by different tubes corresponding to each turn. Fig. 4 shows the FEA model for 3D magnetic field analysis with commercial software, FLUX3D.

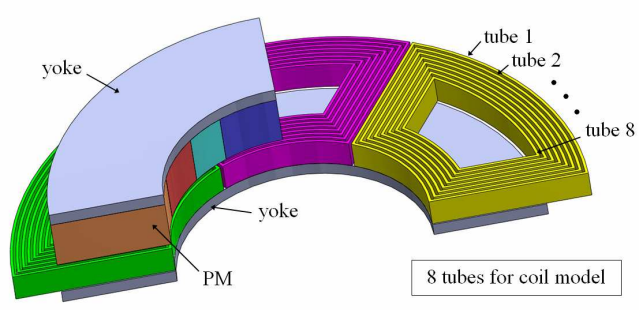

Fig. 4. Analysis model of Model II for FEA method

For the general winding, 3rd and 5th harmonic components of the back EMF are generated as shown in Fig. 5 and Fig. 6. In the results of the SHA, the amplitudes

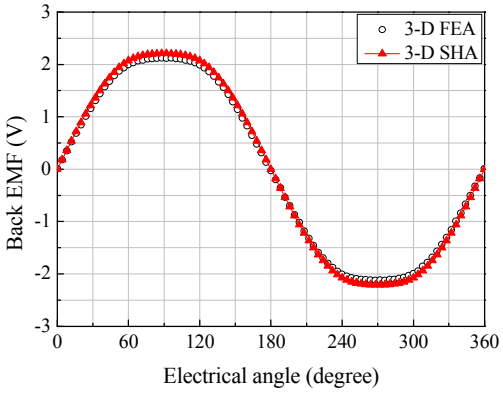

Fig. 5. Comparison of the back EMF waveforms for the general winding layout (@ 7,200 rpm)

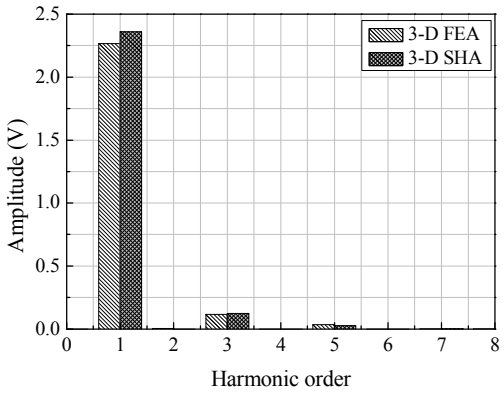

Fig. 6. FFT analysis of the back EMF waveforms for general winding layout (@7,200 rpm)

of the back-EMF have a slightly higher value than those of the FEA. This is due to the leakage flux in the air gap region and partial saturation of core in the FEA analysis.

When input current has pure sinusoidal wave, the 3rd harmonic component of the back EMF in each phase does not influence on the torque ripple in balanced three-phase system. Thus the 3rd harmonic component can be ignored in the design of the back EMF waveform. In this paper, the winding patterns are designed to remove the 5th harmonic of the back EMF waveform.

Fig. 7 shows the procedure of the winding design for Coil I and Coil II corresponding to each method presented in the previous section. In order to remove the 5th harmonic component in the back EMF, the value of kw_5 is made zero by considering up to the 11th order of harmonics in the winding distribution based on (20).

$$kw_5 = \sum_{k=1,3,5\cdots}^{11} N_{\theta k} k_{k5} = (N_{\theta 1} k_{1,5} + N_{\theta 3} k_{3,5} + \cdots + N_{\theta 11} k_{5,11}) = 0 \quad (20)$$

Table 2. Specifications of an analysis AFPM motor

Symbol	Content	Value
N_l	number of winding layers	5
N	number of turns per layer	8
B_r	remanence [T]	1.20
r_i	inner radius of PM [mm]	5.00
r_o	outer radius of PM [mm]	9.45
l_m	magnet length [mm]	2.00
g	air gap length [mm]	0.20

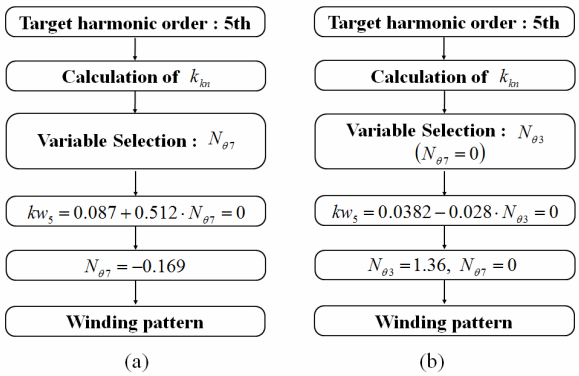

Fig. 7. Procedure of winding design (a) For Coil I (b) For Coil II

For Coil I, it can be done easily by adjusting the 7th harmonic component, $N_{\theta 7}$ of the general winding distribution waveform, because the k_{75} have a biggest value of the k_{k5} as shown in Table 3. Unlike Coil I, in Coil II, the value of 7th harmonic is made to be zero and then the 3rd harmonic of the winding distribution is changed to satisfy (20). Fig. 8 and Fig. 9 show the winding distribution and the winding pattern of general winding, Coil I and Coil II.

Table 3. The value of k_{kn}

n / k	1	3	5	7	9	11
1	0.429	-0.044	0.008	0.004	-0.005	0.002
3	0.139	0.286	-0.028	-0.013	0.015	-0.005
5	-0.072	0.370	0.086	0.027	-0.028	0.009
7	0.049	-0.141	**0.512**	-0.061	0.049	-0.014
9	-0.038	0.092	-0.082	0.490	-0.095	0.022

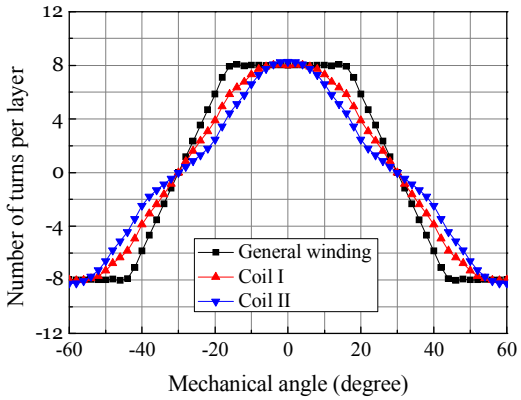

Fig. 8. Winding distributions per layer

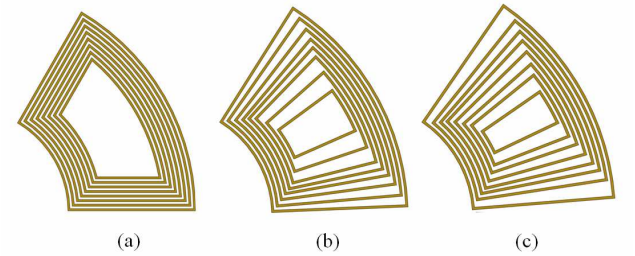

Fig. 9. Winding patterns: (a) General winding; (b) Coil I; (c) Coil II

Fig. 10 and Fig. 11 show the comparison of the back EMF waveforms in SHA and FEA for the Coil I and Coil II respectively. Fig. 12 compares the ratio of the 3rd and 5th harmonic components to fundamental amplitude for the winding distribution. The 5th harmonic component for Coil I and Coil II reduced respectively by 99% and 99% in SHA, and 33% and 80% in FEA as shown in Fig. 12(a). Although the 3rd harmonic component does not have effect on the torque ripple in the balanced three-phase case, it is also decreased in the Coil I and Coil II by 69% and 88% in SHA, and 43% and 62% in FEA respectively as shown in Fig. 12(b).

The difference between the SHA and FEA results in that the PCB winding layout could not accurately express the designed winding distribution. Particularly, the 7th harmonic component of the winding distribution is more difficult to express than the 3rd harmonic. So, the Coil I has much more difference between the analyses results than the Coil II. If the number of turns per layer is enough to

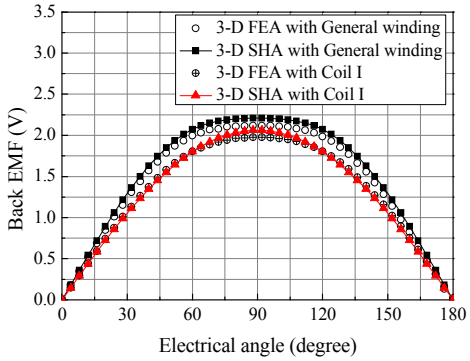

Fig. 10. Comparison of back EMF for Coil I (@7200 rpm)

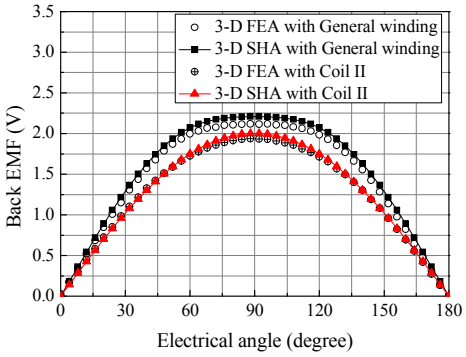

Fig. 11. Comparison of back EMF for Coil II (@7200 rpm)

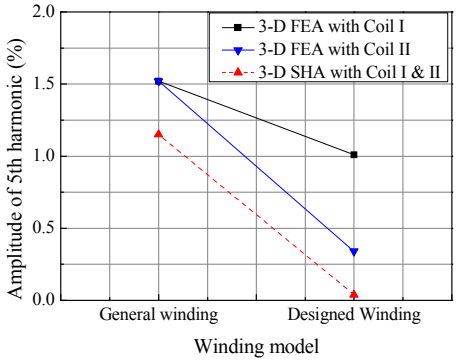

(a)

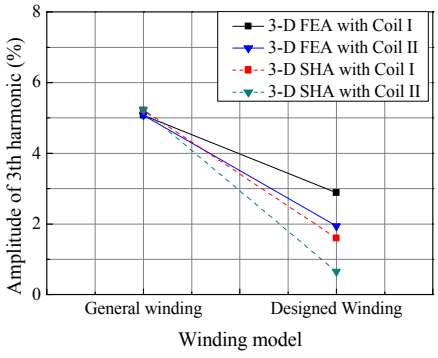

(b)

Fig. 12. Comparison of the amplitude of the harmonics: (a) amplitude of 5th harmonic; (b) amplitude of 3rd harmonic

express the designed winding distribution, it will be more effective to eliminate certain harmonics in the back EMF.

4. Conclusion

This paper deals with a method to control the waveform of the back EMF using PCB windings. For the given PM flux in the air gap region, appropriate winding distribution can be designed to eliminate specific harmonic components in the back EMF by considering the effect of each harmonic in the winding distribution. The proposed method is verified by FEA results and reveals that it can be used to control the shape of the back EMF for better performance of a motor.

Acknowledgements

This work was supported by a grant from the International Cooperation of the Korea Institute of Energy Technology Evaluation and Planning (No. 20102030200011), funded by the Ministry of Knowledge Economy, Republic of Korea.

References

[1] Dr. Duane Hanselman, Brushless Permanent Magnet Motor Design, 2nd ed., The Writers's Collective, 2003, pp. 151-227, 343-366.

[2] M. Markovic and Y. Perriard, "Simplified Design Methodology for a Slotless Brushless DC Motor," *IEEE Trans. Magn.,* vol 42, no 12, 2006, pp 3842-3846.

[3] A.J.A. Vandenput and J. C. Compter, Design and development of a high-speed axial flux permanent-magnet machine, Funda Sahin, 2001, pp. 110-139.

[4] Z. Q. Zhu, D. Howe and C. C. Chan, "Improved analytical model for predicting the magnetic field distribution in brushless permanent magnet machines," IEEE Trans. Magn., vol. 38, no. 1, pp.229-238, Jan. 2002.

[5] T. F. Chan, "Field computation for an Axial Flux permanent-Magnet Synchronous Generator," *IEEE Trans. Magn*., vol 24, no 1, 2009, pp. 1-11.

[6] J. Azzouzi, G. Barakat and B. Dakyo, "Quasi-3D Analytical Modeling of the Magnetic Field of an Axial Flux Permanent Magnets Synchronous Machine", *IEEE Trans. Magn*., vol. 20 no. 4, 2005, pp. 746-752.

Dae-Kyu Jang He received B.S. degree in electrical engineering from Dong-A University, Busan, Rep. of Korea in 2011. Since 2011, he has been studying for M.S. degree in electrical engineering from Dong-A University. His research interests are design and analysis of electro-mechanical systems including driving circuits.

Jung-Hwan Chang He received B.S. and M.S. degrees in electrical engineering and Ph.D. degree in precision mechanical engineering from Hanyang University, Seoul, Rep. of Korea in 1994, 1997 and 2001, respectively. From 2001 to 2002, he worked at Institute of Brain Korea 21 at Hanyang University, where he developed micro drive and high-speed spindle motor. From 2002 to 2003, he worked as research fellow at University of California at Berkeley with the support of Korea Science and Engineering Foundation, and analyzed and developed electrically controlled engine valve system. From 2003 to 2009, he worked in Korea Electrotechnology Research Institute (KERI) as a senior researcher, and engaged in the developments of special purpose machines. Since 2009, he has been with the department of electrical engineering, Dong-A University, Busan Rep. of Korea, as a assistant professor. His interests are the design and analysis of electro-mechanical systems including driving circuits.

Gun-Hee Jang He received Ph. D. degree in Mechanical Engineering from University of California, Berkeley. His research interests are Vibration Analysis of Rotating System, Analysis of Hydrodynamic Bearing and Analysis of Electromechanical Coupled Field in a BLDC Motor.